Analyses of elastically scattered charged pions from calcium isotopes and the ^{48}Ca-^{54}Fe isotone at 180 MeV

Zuhair Fayyad Mahmoud SHEHADEH[*]
Physics Department, Taif University, Taif, Saudi Arabia

Abstract: The elastic scattering of 180 MeV positively and negatively charged pions, incident on a set of calcium isotopes and the isotone ^{48}Ca – ^{54}Fe, has been analyzed within the framework of a recently updated simple local optical potential. This potential, particularly at the tail region, has been originally determined from available phase shifts using inverse scattering theory and the Klein–Gordon equation as a guide. The analysis is carried out with and without considering the squared potential term in the Klein–Gordon equation. Coulomb effects are accounted for by implementing Stricker's prescription. The numerical results for the angular distributions with isotopic and isotonic shifts have been well reproduced. Relative potential differences, in the imaginary part, for $\pi^- - {}^{48}$Ca,^{40}Ca and $\pi^+ - {}^{54}$Fe,^{48}Ca also reveal that the neutron distribution in ^{48}Ca is more extended by about 0.21 fm.

Key words: Pion-nucleus potential, isotopes and isotones, elastic scattering, inverse scattering theory

PACS No. 25.80.Dj, 11.80.-m, 24.10.Ht

1. Introduction

Over the past few decades, it has been scientifically established that the pion's many properties make it the most useful probe to study features of strong interactions. As it is now well known, meson factories such as LAMPF, SIN, and TRIUMF provided a great deal of high-precision pion-nucleus elastic scattering data, spanning a wide range of targets over many energy regions. Many theoretical models [1,2] were developed to analyze early data, but many of them had problems accounting for subsequent data.

Twenty years ago, Satchler [3] introduced a local potential of the Woods–Saxon type to describe the elastic scattering of pions from nuclei in the delta resonance region. Satchler's potential was determined by reducing the relativistic Klein–Gordon equation by neglecting the squared term of the potential, $V^2/2E$, to the nonrelativistic Schrödinger equation and by redefining the mass and energy of the incident pion. The simplicity and success of this type of potential determined using this artifact was striking. Despite its remarkable success, however, it fails to describe large-angle data well [4]. In fact, many theorists, therefore, have used Satchler's potential in studying pion-nucleus scattering [5] only at angles of less than $80°$.

Recently, Shehadeh et al. [6] developed an inverse scattering theory at a fixed energy to determine the nature of pion-nucleus optical potential. The inverse scattering theory at a fixed energy enunciated in that work, which will not be included here, was used in determining the potential from the phase shift analyses of Fröhlich et al. [7] at different incident pion energies. The deduced potential, using inverse scattering theory and

[*]Correspondence: zfs07@hotmail.com

the full Klein–Gordon potential, shows remarkable success [8] in accounting for the experimental cross-sections at all angles.

Here, the elastically scattered pions of both positive and negative charges from ^{40}Ca and its isotopes and from ^{54}Fe, at 180 MeV [9], will be analyzed. The choice of this energy, $T_\pi = 180$ MeV, is feasible since all needed experimental measurements are available and the success of different theoretical models used to analyze these data was marginal. A major importance of using these nuclei is to see the effect of proton and neutron excesses on the parameters of the potential. In addition, the strength of our potential will be reexamined in accounting for isotopic and isotonic shifts in the differential cross-sections, and for the total reaction cross-sections. To account for Coulomb effects, Stricker's empirical treatment [10] will be used. The strategy of the Stricker treatment is based on the following observation: when a negative pion approaches the nucleus it is accelerated by the Coulomb field, whereas a positive pion is decelerated. Stricker argued that the increasing and decreasing effect of Coulomb potential could be incorporated by increasing and decreasing the kinetic energy of π^- and π^+ by the barrier height, respectively. The latter is 7.6 MeV for ^{40}Ca and 8.5 MeV for ^{54}Fe. In this treatment, we adopt his values. As such, this treatment requires no recasting in our equations. Furthermore, our most recent analyses [11] have proven the success of our potential in explaining the $\pi^\pm - ^{40}$Ca elastic scattering data in the delta resonance energy region. In Section 2, we present the methodology of this work. Section 3 provides the results and discussion, and the conclusions are presented in Section 4.

2. Methodology

In nuclear physics, it is well known that the interaction between the pion and the target nucleus is represented by a potential that depends on the relative distance r relating the position of the pion to the center-of-mass of the nucleus. This potential is then inserted into the Klein–Gordon equation for spinless relativistic cases.

The analytical form of the local optical potential, which was extracted from pion-calcium available phase shifts using the inverse scattering theory as a guide and the full Klein–Gordon equation, has the following form [12].

$$V(r) = \frac{V_o}{1 + \exp\left(\frac{r-R_o}{a_o}\right)} + \frac{V_1}{\left[1 + \exp\left(\frac{r-R_1}{a_1}\right)\right]^2} + i\frac{W_2}{1 + \exp\left(\frac{r-R_2}{a_2}\right)} + i\frac{W_3 \exp\left(\frac{r-R_3}{a_3}\right)}{\left[1 + \exp\left(\frac{r-R_3}{a_3}\right)\right]^2} \tag{1}$$

Since the potential is spherically symmetric, the radial part of the Klein–Gordon wave function, $R_{nl}(r)$, satisfies the following equation:

$$\left[d^2/dr^2 + k^2 - U(r) - \frac{l(l+1)}{r^2}\right] R_{nl}(r) = 0, \tag{2}$$

where $R_{nl}(r)$ is r times the radial part of the wave function for a spherical symmetric external potential. Additionally, in Eq. (2), k^2 and $U(r)$ are given by:

$$k^2 = \left(E^2 - m^2c^4\right)/\hbar^2c^2, \tag{3}$$

$$U(r) = \frac{2E}{\hbar^2c^2}\left[V(r) - V^2(r)/2E\right]. \tag{4}$$

In Eq. (3), E and m are, respectively, the effective pion energy and effective pion mass calculated by following Satchler's relativistic correction treatment, and c is the velocity of an electromagnetic wave in vacuum. $V(r)$ is the complex pion-nucleus potential.

As is well known, the scattering amplitude $f(\theta)$, at an angle of θ in the center-of-mass system, is given by [13] :

$$f(\theta) = f_c(\theta) + \frac{1}{2ik} \sum_{\ell=0}^{\infty} (2\ell + 1) \exp(2i\sigma_\ell) [\exp(2i\delta_\ell) - 1] P_\ell(\cos\theta), \qquad (5)$$

where $f_c(\theta)$ is the point Coulomb scattering amplitude, σ_ℓ is the point Coulomb phase shift, δ_ℓ is the complex nuclear phase shifts, and $P_\ell(\cos\theta)$ is the Legendre polynomial.

The differential cross-section for elastic scattering can then be given by:

$$\frac{d\sigma}{d\Omega} = |f(\theta)|^2. \qquad (6)$$

For relativistic scattering of charged particles $V_c \neq 0$, and the Coulomb part must be considered in the Klein–Gordon equation. This is well known to have a major effect on the asymptotic solution, especially with considering the term quadratic in the Coulomb potential. The reason behind that is the interplay between this term and the centrifugal barrier term. Both terms behaves as $1/r^2$ asymptotically.

Following Pilkuhn [14], an expression for the scattering amplitude for the Klein–Gordon equation with the Coulomb potential was determined in [15] and [16]. This has a form similar to that for the nonrelativistic case but with noninteger ℓ-values and complex gamma functions.

In a recent work, Shehadeh et al. [15] compared the results using this scattering amplitude with those using Stricker's treatment along with experimental values. The results obtained in both cases agreed quite well over the entire angular distribution for π^+ scattered elastically by ^{40}Ca. As such, Stricker's assumption has been used in this study to account for the Coulomb part in the Klein–Gordon equation.

3. Results and discussion

The parameters of the real and imaginary parts of the potential for the scattering of positive and negative pions from the calcium isotopes $\left(^{40}_{20}Ca,\ ^{44}_{20}Ca,\ ^{48}_{20}Ca\right)$ and the $^{48}_{20}Ca, ^{54}_{26}Fe$ isotones that give reasonable fits to the observed angular distributions at $T_\pi = 180$ MeV are listed in the Table.

Table. The potential parameters V_o (in MeV), R_o (in fm), a_o (in fm), V_1 (in MeV), R_1 (in fm), a_1 (in fm), W_2 (in MeV), R_2 (in fm), a_2 (in fm), W_3 (in MeV), R_3 (in fm), and a_3 (in fm), used in Eq. (1) for the 180 MeV incident-energy charged pions at calcium isotopes and isotones. The blank entries indicate that the parameters are unchanged.

Target	Pion	V_o	R_o	a_o	V_1	R_1	a_1	W_2	R_2	a_2	W_3	R_3	A_3
$^{40}_{20}Ca$	π^+	33.5	4.669	0.053	580	2.5	0.563	250	3.151	0.330	211.6	3.137	0.70
	π^-											2.937	
$^{44}_{20}Ca$	π^+											3.137	
	π^-											3.137	
$^{48}_{20}Ca$	π^+											3.137	
	π^-											3.337	
$^{54}_{26}Fe$	π^+											3.537	
	π^-											3.537	

The real and imaginary parts of the potential for ^{40}Ca derived from the inverse scattering theory are shown as solid dots in Figure 1. The solid lines represent the real and imaginary parts of the potential used in

fitting the $\pi^{\pm} - {}^{40}$Ca data. As is well known, the inverse scattering method is most reliable in determining the exterior of the potential, which is the case here. Unfortunately, and to the best of our knowledge, no available phase shifts for pion ^{44}Ca, ^{48}Ca, and ^{54}Fe cases exist. However, it is interesting that the π^{+} and π^{-} elastic data at 180 MeV incident energy can be fitted very well by changing the absorption slightly.
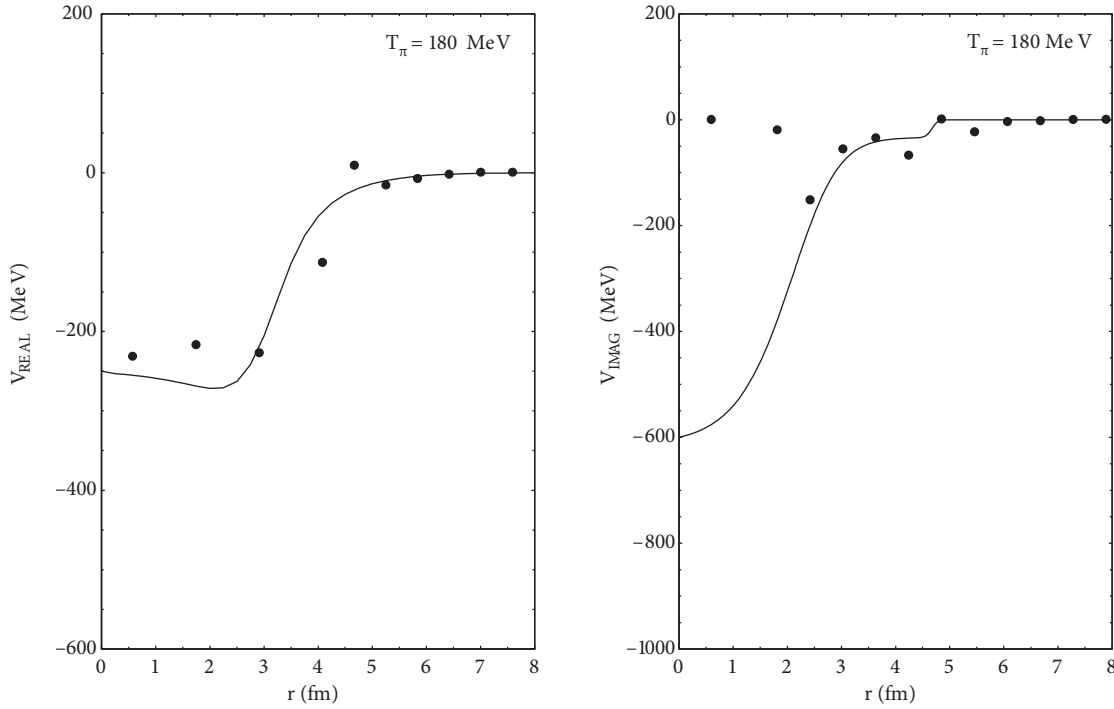

Figure 1. The real and imaginary parts of our potential (solid lines), given by Eq. (1) with the parameters listed in the Table, are compared with the potential points (solid dots) extracted from available phase shifts using inverse scattering theory.

The agreement between our calculated angular distributions, represented by solid lines neglecting the squared term of the potential and dashed lines including the squared term, and observed (solid circles) angular distributions [17], shown in the Figures 2–5, is excellent. It is worth noticing, as the Table shows, that the slight and systematic change is only in one free parameter, namely the absorption radius, R_3. One may also notice that our calculated reaction cross-sections, which are 886 and 951 mb for the $\pi^{+} - {}^{40}$Ca and $\pi^{-} - {}^{40}$Ca cases, respectively, agree very well with the ones published by Akhter et al. [18] and underestimate the calculated values by others [19]. It is also impressive to see the good agreement between the calculated angular distributions, with and without the squared potential term, and the available experimental data at forward angles. Nevertheless, our calculations predicted the angular distributions at backward angles. As such, good accurate data at large angles are needed. This could be significant in determining the correct potential.

To show the effect of neutron and proton excesses on the scattering of negative and positive pions, respectively, the relative potential differences have been calculated from the (^{48}Ca, ^{40}Ca) isotope and (^{54}Fe, ^{48}Ca) isotone, and the corresponding graphs are shown in Figure 6.

In Figure 6, it is clear that the maximum for the neutron excess case $\left({}^{48}_{20}\text{Ca}, {}^{40}_{20}\text{Ca}\right)$ occurs at a radius smaller than that for the proton excess case $\left({}^{54}_{26}\text{Fe}, {}^{48}_{20}\text{Ca}\right)$ by about 0.21 fm, but the maximum values are the
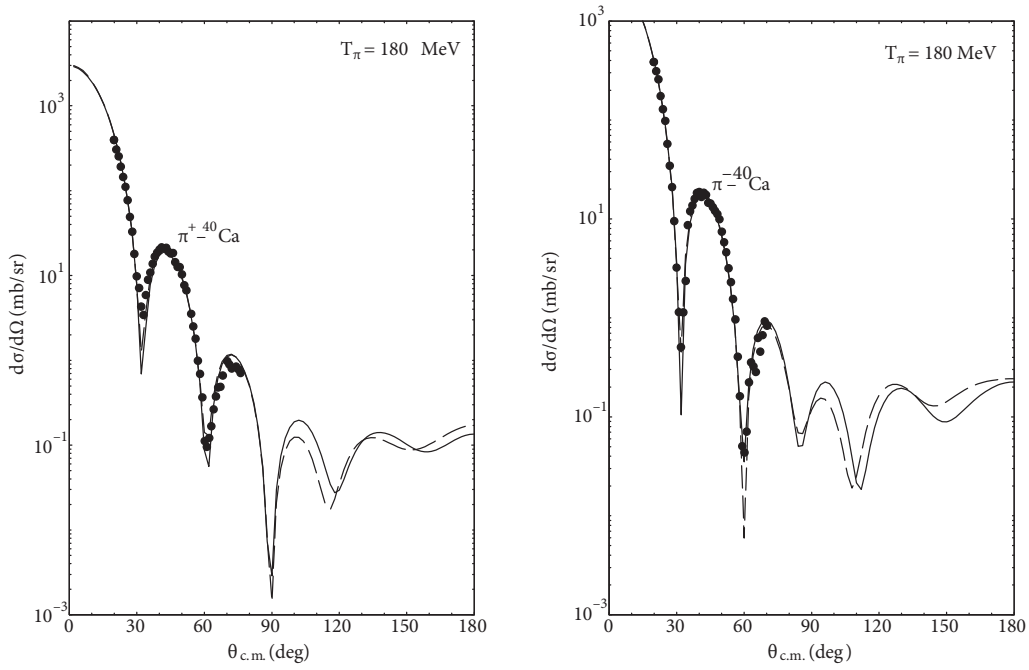
Figure 2. The angular distributions (solid line and dashed line, without and including the squared term of the potential, respectively) obtained by using our potential with the parameters listed in the Table are compared with the observed angular distributions [9] (solid circles) for the scattered charged pions from ^{40}Ca.
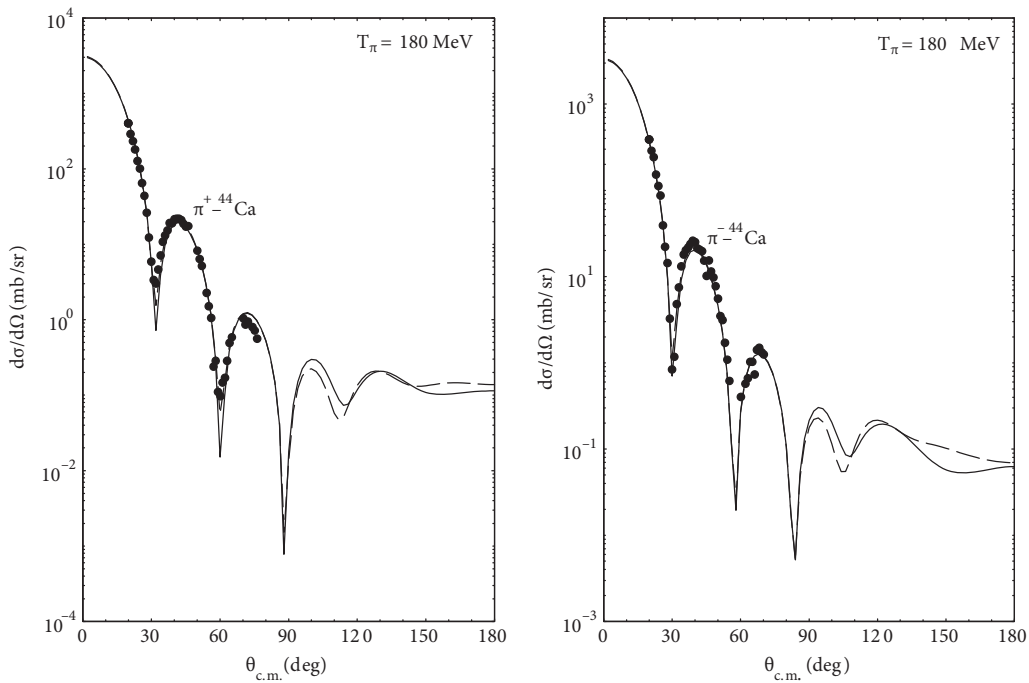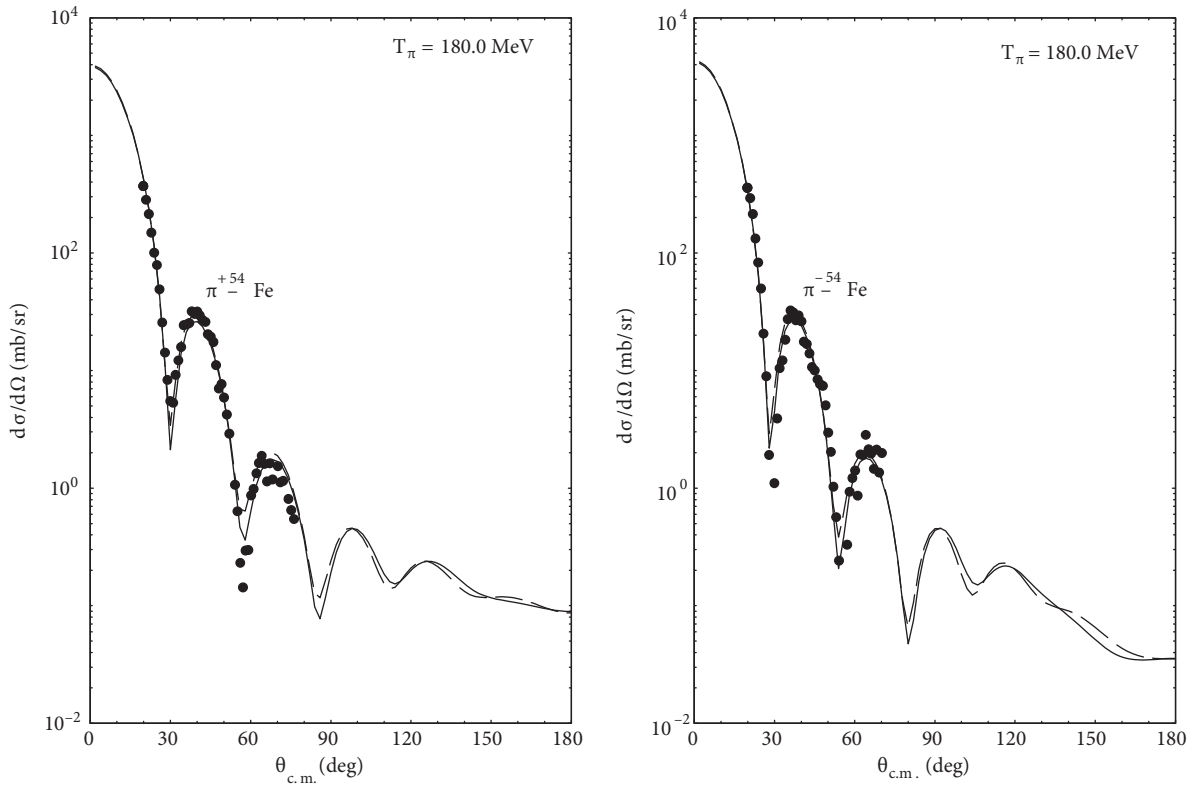

Figure 3. Same as Figure 2, but for ^{44}Ca.

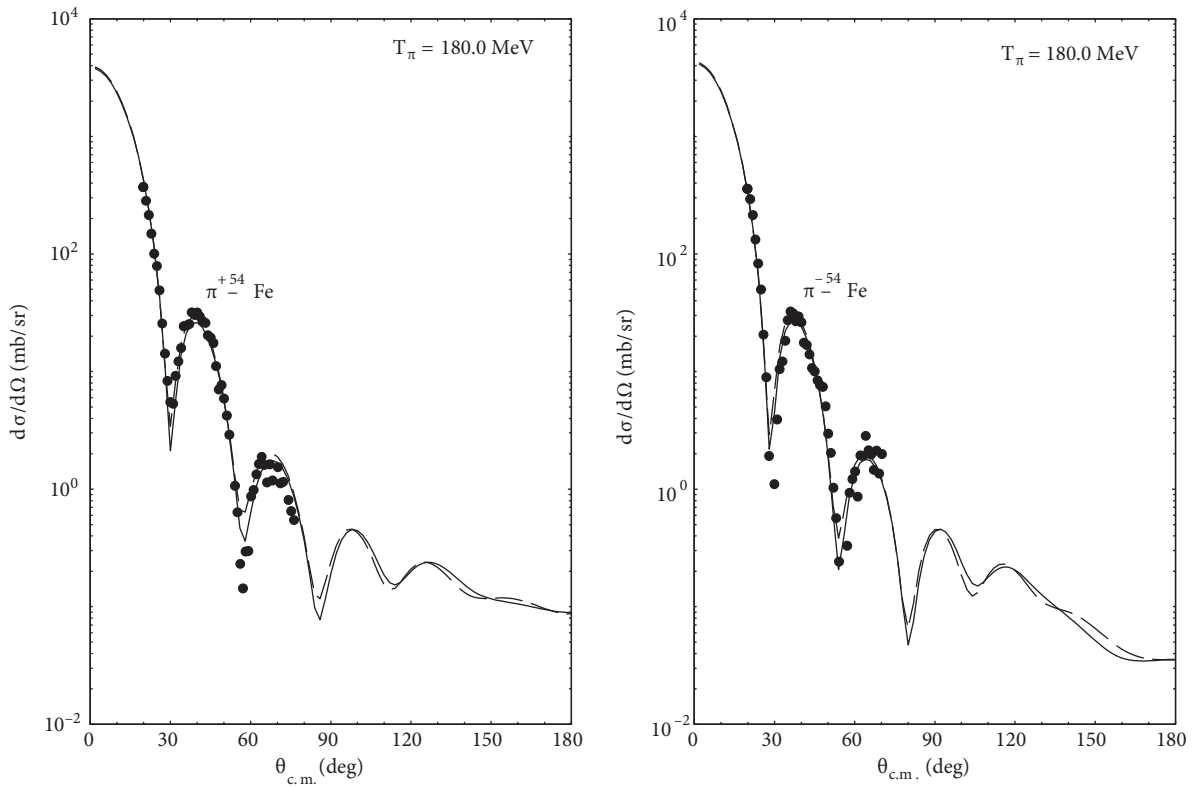**Figure 4.** Same as Figure 2, but for ^{48}Ca.

Figure 5. Same as Figure 2, but for ^{54}Fe.

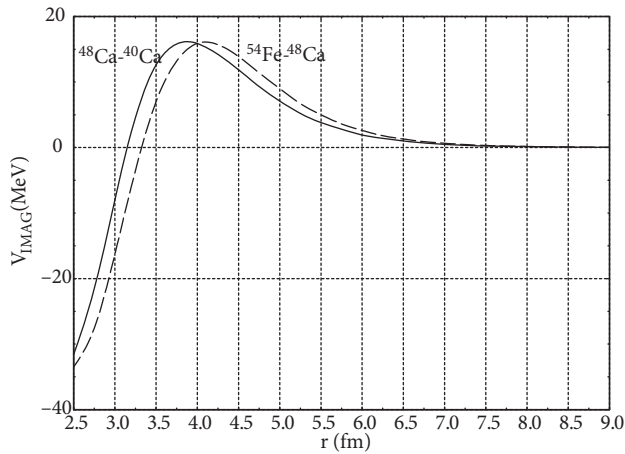**Figure 6.** Comparison between the relative potential difference (the absorption part) for $\pi^- - {}^{48}Ca$, ${}^{40}Ca$ (solid curve) and $\pi^+ - {}^{54}Fe$, ^{48}Ca (dashed curve). The peaks indicate that π^- favors the interaction with neutrons while π^+ favors that with protons. The shift in the peaks is due to the difference in the neutron and charge root-mean-square radii.

same. This result agrees with that obtained by Boyer [9] and differs from the value reported by Akhter et al. [18]. The result is also closer to that predicted by Hartree–Fock calculations than the one obtained by shell-model calculations [19]. In addition, it is greater than the one calculated for oxygen isotopes [20,21], as it should be.

4. Conclusions

The present work confirms the success of our recently updated potential in explaining, for the first time, the elastic scattering of charged pions from calcium isotopes and the ${}^{48}Ca - {}^{54}$Fe isotone at 180 MeV incident energy. It is nice that this has been achieved by a systematic change in only one parameter, R_3. Isotopic and isotonic shifts in the angular distributions are also well reproduced. The calculated angular distributions, with and without squared potential term in the Klein–Gordon equation, show a remarkable agreement with the measured values available at forward angles. They differ, however, at large angles. Precise large angle data are needed and may be crucial in determining the true nature of the potentials. In addition, this study confirms that neutron distribution in ^{48}Ca is more extended by 0.21 fm, i.e. $r_n^{48} - r_n^{40} \approx 0.21 fm$.

Acknowledgment

References

[1] T. S. Lee and R. Redwine, *Ann. Rev. Nuc. Part. Sci.*, **52**, (2002), 23.

[2] T. Ericson and W. Weise, Pions and Nuclei (Claredon, Oxford. 1988).

[3] G. Satchler, *Nucl. Phys. A*, **540**, (1992), 533.

[4] Z. Shehadeh, M. Sabra and F. Malik, *Condens. Matter Theor.*, **18**, (2003), 339.

[5] S. A. Khallaf and A. Ebrahim, *Phys. Rev. C*, **62**, (2000), 024603-1.

[6] Z. Shehadeh, M. Alam and F. Malik, *Phys. Rev. C*, **59**, (1999), 826.

[7] J. Fröhlich, H. Pilkuhn and H. Schlaile, *Nucl. Phys. A*, **415**, (1984), 399.

[8] Z. Shehadeh, *Int. J. Mod. Phys. E*, **18**, (2009), 1615.

[9] K. Boyer, PhD Thesis, Department of Physics, The University of Texas at Austin, Texas, USA, 1983.

[10] K. Stricker, PhD Thesis, Department of Physics, Michigan State University, Michigan, USA, 1979.

[11] Z. Shehadeh, J. Scott and F. Malik, *Fifth Saudi Physical Society Meeting* (25-27 October 2010), King Khalid University, Abha, Saudi Arabia.

[12] Z. Shehadeh, PhD Thesis, Department of Physics, Southern Illinois University, Illinois, USA, 1995.

[13] K. Krane, Introductory Nuclear Physics (John Wiley & Sons, New York. 1988).

[14] H. Pilkuhn, Relativistic Particle Physics (Springer-Verlag, New York. 1979).

[15] Z. Shehadeh, J. Scott and F. Malik, *Am. Inst. Phys. J.*, (2011), 185.

[16] J. Scott, PhD Thesis, Department of Physics, Southern Illinois University, Illinois, USA, 2012.

[17] R. Freedman, G. Miller and E. Henley, *Phys. Lett.*, **103B**, (1981), 397.

[18] Md. Akhter, S. Sultana, H. Sen Gupta and R. Petersen, *J. Phys. G.: Nucl. Part. Phys.*, **27**, (2001), 755.

[19] J. P. Egger, R. Corfu, P. Gretillat, C. Lunke, J. Piffaretti, E. Schwarz, C. Perrin, J. Jansen and B. Preedom, *Phys. Rev. Lett.*, **39**, (1977), 1608.

[20] J. Dedonder, J. Maillet and C. Schmit, *Ann. Phys.*, **127**, (1979), 1.

[21] C. Ingram, *AIP Con. Proc.*, **54**, (1979), 455.